Title

Ca2+ Influx via the Na+/Ca2+ Exchanger Is Enhanced in Malignant Hyperthermia Skeletal Muscle*

Journal

Journal of Biological Chemistry, 289(27)

ISSN

0021-9258

Authors

Altamirano, Francisco
Eltit, José M
Robin, Gaëlle
et al.

Publication Date

2014-07-01

DOI

10.1074/jbc.m114.550764

Peer reviewed

THE JOURNAL OF BIOLOGICAL CHEMISTRY VOL. 289, NO. 27, pp. 19180–19190, July 4, 2014

Ca^{2+} Influx via the Na^+/Ca^{2+} Exchanger Is Enhanced in Malignant Hyperthermia Skeletal Muscle*

Received for publication, January 16, 2014, and in revised form, May 7, 2014 Published, JBC Papers in Press, May 20, 2014, DOI 10.1074/jbc.M114.550764

Francisco Altamirano[‡], José M. Eltit[§¶], Gaëlle Robin[‡], Nancy Linares[‖], Xudong Ding[§1], Isaac N. Pessah[‡], Paul D. Allen[‡§], and José R. López[‡§‖2]

From the [‡]Department of Molecular Biosciences, School of Veterinary Medicine, University of California, Davis, California 95616, the [‖]Centro de Biofísica y Bioquímica, Instituto Venezolano de Investigaciones Científicas, Caracas 1020-A, Venezuela, the [§]Department of Anesthesiology Perioperative and Pain Medicine, Brigham & Women's Hospital, Boston, Massachusetts 02115, and the [¶]Department of Physiology and Biophysics, Virginia Commonwealth University, Richmond, Virginia 23298

Background: Dysregulation of Ca^{2+} homeostasis have been described in malignant hyperthermia (MH).
Results: Na^+/Ca^{2+} exchanger (NCX3) reverse mode activity is enhanced in MH muscles and it contributes to resting intracellular calcium concentration and Ca^{2+} transients induced by high $[K^+]_e$ and by halothane.
Conclusion: NCX3 reverse mode activity is increased in MH muscle.
Significance: Understanding mechanisms influencing Ca^{2+} dynamics in MH muscle.

Malignant hyperthermia (MH) is potentially fatal pharmacogenetic disorder of skeletal muscle caused by intracellular Ca^{2+} dysregulation. NCX is a bidirectional transporter that effluxes (*forward mode*) or influxes (*reverse mode*) Ca^{2+} depending on cellular activity. Resting intracellular calcium ($[Ca^{2+}]_r$) and sodium ($[Na^+]_r$) concentrations are elevated in MH susceptible (MHS) swine and murine muscles compared with their normal (MHN) counterparts, although the contribution of NCX is unclear. Lowering $[Na^+]_e$ elevates $[Ca^{2+}]_r$ in both MHN and MHS swine muscle fibers and it is prevented by removal of extracellular Ca^{2+} or reduced by t-tubule disruption, in both genotypes. KB-R7943, a nonselective NCX3 blocker, reduced $[Ca^{2+}]_r$ in both swine and murine MHN and MHS muscle fibers at rest and decreased the magnitude of the elevation of $[Ca^{2+}]_r$ observed in MHS fibers after exposure to halothane. YM-244769, a high affinity reverse mode NCX3 blocker, reduces $[Ca^{2+}]_r$ in MHS muscle fibers and decreases the amplitude of $[Ca^{2+}]_r$ rise triggered by halothane, but had no effect on $[Ca^{2+}]_r$ in MHN muscle. In addition, YM-244769 reduced the peak and area under the curve of the Ca^{2+} transient elicited by high $[K^+]_e$ and increased its rate of decay in MHS muscle fibers. siRNA knockdown of NCX3 in MHS myotubes reduced $[Ca^{2+}]_r$ and the Ca^{2+} transient area induced by high $[K^+]_e$. These results demonstrate a functional NCX3 in skeletal muscle whose activity is enhanced in MHS. Moreover reverse mode NCX3 contributes to the Ca^{2+} transients associated with K^+-induced depolarization and the halothane-triggered MH episode in MHS muscle fibers.

The plasma membrane Na^+/Ca^{2+} exchanger (NCX)[3] is a bidirectional electrogenic ($3\ Na^+/1Ca^{2+}$), and voltage-sensitive reversible ion countertransporter, which is mainly responsible for Ca^{2+} extrusion in a variety of cells (1, 2). The activity and direction of NCX transport is driven by the membrane potential (V_m) as well as the transmembrane electrochemical gradients of Na^+ and Ca^{2+} (2). This transporter operates as a high capacity and low affinity system for Ca^{2+} transport, extruding Ca^{2+} against its transmembrane electrochemical gradient coupled to Na^+ influx (*forward mode*), or transporting Ca^{2+} into cells coupled to Na^+ efflux (*reverse mode*) (2).

Three mammalian isoforms of the NCX protein have been discovered (NCX1, NCX2, and NCX3) (3–5). Only the NCX1 and NCX3 isoforms are expressed in skeletal muscle and are localized in the transverse tubules (t-tubules) and in the sarcolemma (4, 6, 7). NCX1 is expressed at high levels during embryonic development and postnatal maturation (8) then its expression is gradually reduced as the NCX3 gene becomes more highly expressed and predominates in adult skeletal muscle (8).

Na^+-dependent Ca^{2+} fluxes have been reported in amphibian skeletal muscle (9, 10), and human myotubes (7). NCX has been observed in sarcolemmal fractions isolated from mammalian muscles (11) and in t-tubules isolated from amphibian muscles (12, 13). In addition, the reverse mode of the exchanger seems to mediate the enhancement of contraction that takes place after external Na^+ withdrawal in phasic and tonic amphibian skeletal muscle fibers (14–17). However, the role of the NCX in skeletal muscle is still controversial and its role in the MHS skeletal muscle fibers is totally unknown.

* This work was supported, in whole or in part, by National Institutes of Health Grants AR43140 (to P. D. A., J. R. L., and I. N. P.), AR052534 (to P. D. A. and J. R. L.), and 4P42 ES04699 (to I. N. P.).
[1] Present address: Dept. of Anesthesia, Shengjing Hospital, China Medical University, Liaoning 110004, China.
[2] To whom correspondence should be addressed: Dept. of Molecular Biosciences, University of California Davis, 1089 Vet Medical Dr., Davis, CA 95616. Tel.: 530-752-3229; Fax: 530-752-4698; E-mail: jrlopez@ucdavis.edu.

[3] The abbreviations used are: NCX, Na^+/Ca^{2+} exchanger; MH, malignant hyperthermia; MHN, non-susceptible to MH; MHS, MH susceptible; $[Ca^{2+}]_r$, resting intracellular calcium concentration; $[Na^+]_r$, resting intracellular sodium concentration; V_m, membrane potential; t-tubules, transverse tubules; SR, sarcoplasmic reticulum; RyR1, type-1 ryanodine receptor; FDB, flexor digitorum brevis; NMG, *N*-methyl-D-glucamine-hydrochloride; KB-R7943, 2-(2-(4-(4-nitrobenzyloxy)phenyl)ethyl)-isothiourea methane sulfonate); YM-244769, *N*-(3-aminobenzyl)-6-{4-[(3-fluorobenzyl)oxy]phenoxy}nicotinamide; TRPC, transient receptor potential channels.

MH is a life-threatening pharmacogenetic syndrome, which occurs when susceptible individuals are exposed to triggering agents, such as halogenated inhalation anesthetics and/or depolarizing muscle relaxants (18). MH susceptibility is associated with a dysfunction of regulation of intracellular resting Ca^{2+} concentration ($[Ca^{2+}]_r$) (19–21) and is characterized by the occurrence of a robust increase in $[Ca^{2+}]_r$ in response to exposure to halothane (19, 22, 23). In more than 70% of humans with MH susceptibility (MHS) the trait is linked to one of >185 mutations within *RYR1* located on ch19q13.1, the gene that encodes the type 1 skeletal isoform of the ryanodine receptor (*RYR1*), the primary Ca^{2+} release channel in the sarcoplasmic reticulum (SR) (24). In addition, mutations in *CACNA1S* on ch1q31–32, which codes for $Ca_V1.1$ have also been found in 2% of MHS individuals (25–27).

In the present study, we assessed the NCX activity in skeletal muscle cells from MHN and MHS swine and mice by measuring $[Ca^{2+}]_r$ and $[Na^+]_r$ in response to external sodium withdrawal. In addition, we studied the contribution of NCX on the Ca^{2+} transient associated with sustained membrane depolarization induced by high $[K^+]_e$ and during an *in vivo* MH episode elicited by halothane in murine MHS muscle fibers. In doing so, we demonstrated that the activity of NCX3 is enhanced in MHS muscle cells and that its reverse mode contributes to the Ca^{2+} transients elicited by K^+ depolarization and halothane-induced elevation on intracellular Ca^{2+} in murine muscle fibers.

EXPERIMENTAL PROCEDURES

Biological Preparation—Experiments were conducted: (i) *in vitro*, using intact intercostal muscle biopsies obtained from 16 MHS Poland China (*RYR1* R615C-Homozygous) and 8 MHN Yorkshire swine. MH susceptibility was determined by PCR amplification of *RYR1* exon 10 in genomic DNA and halothane challenge as previously described (28). Muscle biopsy specimens were removed under general anesthesia using non-triggering agents (thiopental 15 mg/kg for induction, NO_2/O_2/fentanyl to anesthetized the animal). After surgical removal, intact muscle biopsy samples were placed in a temperature-controlled dish (37 °C) bubbled with a mixture of 95% O_2 and 5% CO_2, then dissected free of adipose and connective tissue with the aid of a stereo microscope. They were further divided into several small bundles of four to six muscle fibers for the Ca^{2+} measurements. (ii) *In vitro*, Flexor digitorum brevis (FDB) muscle fibers from 3–4-month-old C57BL/6 MHN and congenic heterozygous *RYR1* R163C C57BL/6 MHS mice (29) were obtained by enzymatic digestion. FDB muscles were incubated with 400 units/ml of collagenase type 2 (Worthington, Lakewood, NJ) in DMEM supplemented with penicillin/streptomycin (1 time) for 90 min at 37 °C and 5% CO_2. Muscles were then washed in DMEM and single fibers were mechanically dissociated with progressively smaller fire-polished Pasteur pipettes. Isolated fibers were seeded in ECM-coated 96-well plates in DMEM supplemented with 10% fetal bovine serum and penicillin/streptomycin (1 time) and incubated at 37 °C and 5% CO_2. Fibers were used for experimentation 20–24 h after isolation. (iii) *In vivo*, in vastus lateralis fibers in anesthetized MHN and MHS mice as described previously (18). The institutional animal care committees at the Instituto Venezolano de Investigaciones Científicas, the Harvard Medical Area, and the University of California, Davis, approved all experimental protocols.

Ca^{2+} and Na^+ Selective Microelectrodes—Double-barreled Ca^{2+} selective and Na^+ selective microelectrodes were prepared as described previously (19). The calcium ionophore II, ETH-129 (Fluka, Sigma), and the Na^+ ionophore I, ETH-227 (Fluka, Sigma), were used to back-fill the Ca^{2+} and Na^+-selective microelectrodes, respectively. Each ion-selective microelectrode was individually calibrated as described previously (25, 30). After making measurements of $[Ca^{2+}]_r$ and $[Na^+]_r$ all microelectrodes were recalibrated, and if the two calibration curves did not agree within 3 mV, data from that microelectrode were discarded. The drugs used in the present study did not interfere with Ca^{2+} microelectrode sensitivity in the relevant ranges studied (from *p*Ca6 to *p*Ca7 and from 1 to 30 mM Na^+).

Recording of V_m, $[Ca^{2+}]_r$, and $[Na^+]_r$ in Vitro—Measurements of V_m, $[Ca^{2+}]_r$, and $[Na^+]_r$, were performed on intact intercostal muscle bundles obtained from MHN and MHS swine. The intact muscle bundles were mounted horizontally in a Plexiglas temperature-controlled chamber (International Plastic, Miami, FL) (36 ± 1.5 °C) that was placed on the stage of an upright microscope. Each tendon was fastened to a stainless steel hook connected to micromanipulators and the sarcomere length was adjusted to 2.2 μm using a laser diffraction technique (31). The muscle preparation was perfused continuously with bicarbonate-buffered swine physiologic solution (see below for composition), bubbled with a mixture of 95% O_2 and 5% CO_2, pH 7.4. Individual muscle fibers were impaled with either a double-barreled Ca^{2+} or Na^+ selective microelectrodes and V_m, V_{CaE}, and V_{NaE} potentials were recorded via high impedance amplifier (WPI FD-223 or WPI Duo 773 electrometer; WPI, Sarasota, FL). The potential from the V_m barrel (3 M KCl) was subtracted electronically from V_{CaE} or V_{NaE}, to produce a differential Ca^{2+}-specific (V_{Ca}) or Na^+ specific (V_{Na}) potential that represents $[Ca^{2+}]_r$ or $[Na^+]_r$. V_m, V_{Ca}, and V_{Na} were filtered with a low-pass filter (30–50 KHz) to improve the signal-to-noise ratio and stored in a computer for further analysis.

Recording of V_m, $[Ca^{2+}]_r$, and $[Na^+]_r$ in Vivo—$[Ca^{2+}]_r$ and $[Na^+]_r$ were measured *in vivo* in MHN and MHS mice as described previously (19). In brief, mice were anesthetized with 100 mg/kg of ketamine and 5 mg/kg of xylazine, intubated, and ventilated with air using a mouse ventilator (Harvard Minivent, M-845, Holliston, MA). The mice were kept euthermic (37–37.5 °C) using of a heating pad with an automated feedback loop (ATC-1000 temperature controller, WPI, Sarasota, FL). The vastus lateralis was then exposed surgically and determinations of $[Ca^{2+}]_r$ or $[Na^+]_r$ were made in its superficial fibers. Several muscle fibers in each leg were impaled to measure ion concentrations for each condition in each leg (control condition, after test drug application and after halothane exposure). Halothane (1.5%) was administered using a vaporizer (Kent Scientific Corporation, Torrington, CT) connected to the ventilator in such a way as to prevent backpressure on the vaporizer. The procedure to record V_m, V_{CaE}, and V_{NaE} and to obtain and process the specific potential for Ca^{2+} (V_{Ca}) or Na^+ (V_{Na}) for later analysis was identical to that described above for *in vitro* experiments.

Glycerol Treatment—It is well established that glycerol treatment can be used to osmotically disrupt the transverse tubules in skeletal muscle (32, 33). Briefly, intact MHN and MHS swine muscle fibers were incubated in 350 mM glycerol solution for 1 h, and then returned to normal swine physiologic solution (32). Destruction of the transverse tubular system occurs not in the glycerol solution itself, but occurs only after the muscle fibers have been returned to normal physiologic solution due to the osmotic shock produced by glycerol withdrawal. The osmotic shock produces a physical and functional dissociation of the t-tubules from the surface membrane (detubulation) (32, 33).

Ca^{2+} Imaging—Isolated FDB fibers were loaded in a solution of Fluo4-AM (50 μg vial) dissolved in 20% pluronic acid in DMSO (15 μl), and diluted in murine physiological solution to a final concentration of 10 μM. Dye loading was done at room temperature for 30 min and muscle cells were then washed once with normal murine physiological solution and then transferred to the stage of an IX71 inverted microscope. To prevent motion artifact due to muscle contraction during K^+ depolarization the perfused solution was supplemented with 10 μM *N*-benzyl-*p*-toluene sulfonamide (Sigma).

The experimental protocol used was the following: single muscle fibers were perfused with normal potassium (5 mM K^+) solution for 1 min, then with high potassium (60 mM K^+) solution for 3 min, and then returned to normal (5 mM K^+) solution for another 1 min. To study the contribution of NCX3 reverse mode on K^+ depolarization-induced Ca^{2+} transients, muscle fibers were preincubated with 1 μM YM-244769 for 5 min and then used at the same depolarization protocol as described above (1 μM YM-244769 was added to all the solutions).

For measurements of Ca^{2+} transients, fibers were illuminated at 494 nm to excite Fluo-4 with a DeltaRam wavelength-selectable light source. Fluorescence emission at 510 nm was captured from individual muscle fibers at 20 frames/s using a Cascade Evolve 512 camera (Photometrics, Tucson, AZ). The images were acquired using the Easy Ratio Pro software (PTI). Fluorescence data (F) were normalized to the fluorescence base line (F_o) of each individual fiber and expressed as $(F - F_0)/F_0$ or $\Delta F/F_0$. The data were analyzed using Prism 6 software (GraphPad Software, Inc.). Peak amplitude and area under the curve within the evoked responses was calculated from the number of fibers indicated in the bar graphs. Rates of decay (k) were calculated adjusting the curve to a single exponential decay function ($y(t) = y_o \cdot e^{-kt}$).

Myotubes Culture and Transfection—Primary myoblasts were isolated from the hindlimb and forelimb muscles of neonatal MHS (R163C Het) mice and their MHN (C57BL/6) littermates (34). Myoblasts were differentiated for 3 days into myotubes by withdrawal of growth factors as described previously (34). Myoblasts were placed in DMEM low glucose 5% horse serum and 1× penicillin/streptomycin/glutamine for 1 day and the transfected with either scramble FITC siRNA or NCX3 siRNA (a pool of 3 target-specific 19–25-nucleotide siRNAs, Santa Cruz Biotechnology) and scramble FITC siRNA (25 nM) with DharmaFECT 1 transfection reagent (Thermo Scientific) for 1 day at 37 °C in DMEM low glucose 5% horse serum without antibiotics according to the manufacturer's instructions. Media was changed after 1 day (with antibiotics) and myotubes were differentiated for another day (total 3 days of differentiation). Myotubes were then loaded with 5 μM Fura2-AM for 30 min at room temperature and calcium transients were assessed with high potassium solution as described above. FITC fluorescence channel was used to select transfected myotubes to carry out the experiments. $[Ca^{2+}]_r$ was assessed by Ca^{2+} selective microelectrodes as described above. Total myotubes lysates were analyzed by standard Western blot technique 48 h after transfection (see below).

Measurement of SR Ca^{2+} Loading in MHN and MHS Adult Fibers and Myotubes—Adult FDB fibers were loaded with Fluo-4AM and incubated with *N*-benzyl-*p*-toluene sulfonamide to avoid contraction artifacts. SR Ca^{2+} loading was measured using the area under the curve following a 30-s exposure to 20 mM caffeine in Ca^{2+}-free media (+1 mM EGTA). Myotubes were loaded with Fluo-4AM. SR Ca^{2+} loading was evaluated by measuring the area under the curve of the Ca^{2+} transient evoked by a 60-s exposure to 5 μM ionomycin in Ca^{2+}-free media (+1 mM EGTA). To test the effect of YM-244769 on SR Ca^{2+} loading both adult FDB fibers and myotubes were incubated for 5 min with 1 μM YM-244769 and this concentration was maintained constant during exposure to either caffeine or ionomycin.

Western Blot—Quadriceps muscles were dissected and minced to smaller pieces with a pair of scissors and then homogenized with an electric homogenizer in modified RIPA buffer (150 mM NaCl, 50 mM Tris, pH 7.4, 1% Triton X-100, 0.5% sodium deoxycholate, 0.1% SDS, 5 mM EDTA, 2 mM EGTA, 1× Roche Complete protease inhibitor). Myotubes were scraped in modified RIPA buffer. Lysates were incubated for 30 min on ice and then spun down by centrifugation at 16,000 × *g* for 20 min at 4 °C. Protein concentrations were determined using the BCA method (Thermo Scientific). Proteins (50 μg) were separated using SDS-PAGE 4–15% gradient gels (Bio-Rad) and transferred to PVDF membranes. The PVDF membranes were blocked with SEA Blocking Buffer, 0.1% Tween 20 (Thermo Scientific), incubated overnight at 4 °C with NCX3 (Alpha Diagnostic International, 1:1000) and GAPDH (Santa Cruz Biotechnology, 1:5000) antibodies in blocking buffer, and then washed with PBS, 0.1% Tween 20 (PBS-T). After washing they were incubated with the secondary antibodies in blocking buffer (IRDye 680 and 800 nm, Li-COR Biosciences) for 1 h, then washed with PBS-T and quantified with Odyssey Imaging System (Li-COR Biosciences).

Equilibrium Potential Calculations—Equilibrium potentials were calculated by Nernst equation (Equation 1), using the results obtained in this work, as follows.

$$E_{ion} = -\frac{RT}{zF}\ln\frac{[ion]_i}{[ion]_e}$$

$$E_{Na^+} = -61\log\frac{[Na^+]_i}{[Na^+]_e} \qquad \text{(Eq. 1)}$$

$$E_{Ca^{2+}} = -30.5\log\frac{[Ca^{2+}]_i}{[Ca^{2+}]_e}$$

$[Na^+]_e$ for swine was 130 mM and for murine was 140 mM. $[Ca^{2+}]_e$ was 2.5 mM. V_m, $[Ca^{2+}]_r$, and $[Na^+]_r$ values are

described under "Results" and summarized in Table 1. Reverse potentials for NCX were calculated with Equation 2.

$$E_{NCX} = 3E_{Na^+} - 2E_{Ca^{2+}} \quad \text{(Eq. 2)}$$

Solutions—Swine physiologic solution had the following composition (in mM): 130 NaCl, 5 KCl, 2.5 $CaCl_2$, 1 $MgCl_2$, 18 $NaHCO_3$, 1 NaH_2PO_4, and 5 glucose. The pH was 7.4 when it was aerated with a mixture of 5% CO_2 and 95% O_2. Low or Na^+-free solution was prepared by partial or total withdrawal of $[Na^+]_e$, which was replaced by an equivalent amount by *N*-methyl-D-glucamine (NMG) hydrochloride to maintain osmolarity. Ca^{2+}-free solution was prepared by omitting the $CaCl_2$ and adding 1 mM EGTA and 2 mM $MgCl_2$.

The composition of murine physiologic solution was (in mM): 140 NaCl, 5 KCl, 2.5 $CaCl_2$, 1 $MgSO_4$, 5 glucose, and 10 HEPES, pH 7.4. Glycerol, 2-(2-(4-(4-nitrobenzyloxy) phenyl)ethyl)-isothiourea methane sulfonate) (KB-R7943), or *N*-(3-aminobenzyl)-6-{4-[(3-fluorobenzyl)oxy]phenoxy}nicotinamide (YM-244769) solutions were made by adding the desired concentration of the reagent to normal physiologic solution. High potassium (60 mM K^+) solution was prepared by equimolar replacement of NaCl by KCl. The NaCl concentrations were adjusted to maintain a total ionic strength $[Na^+] + [K^+]$ constant at 145 mM.

Statistical Analysis—All values are expressed as mean ± S.E. and *n* is equivalent to the number of independent measurements. Statistical analysis was performed using unpaired *t* test, or one-way analysis coupled with Tukey's *t* test for multiple measurements to determine significance ($p < 0.05$).

RESULTS

$[Ca^{2+}]_r$ and $[Na^+]_r$ Are Elevated in Swine MHS Muscle Fibers—As we have described previously (22) $[Ca^{2+}]_r$ in swine MHS muscle fibers was 3-fold higher than in MHN muscles (374 ± 5 *versus* 119 ± 1 nM, $n = 25$, $p < 0.001$) with no significant changes in resting membrane potential (−82 ± 0.1 *versus* −82 ± 0.4 mV, $n = 25$, $p > 0.05$) between the two groups. Similarly, $[Na^+]_r$ was elevated 2-fold in MHS compared with MHN fibers (16.4 ± 0.2 *versus* 8.0 ± 0.1 mM, $n = 25$, $p < 0.001$).

Na^+ Withdrawal Increased $[Ca^{2+}]_r$ in Muscle Fibers—To explore the NCX reverse mode activity in MHN and MHS swine muscle fibers Na^+ was replaced in equivalent amounts by the impermeant cation NMG. Lowering $[Na^+]_e$ caused an increase of $[Ca^{2+}]_r$ in both MHN and MHS swine muscle fibers. In MHN muscle fibers $[Ca^{2+}]_r$ increased from 119 ± 1 to 213 ± 3 nM when $[Na^+]_e$ was reduced from 130 to 65 mM, and rose to 382 ± 5 nM when external Na^+ was completely removed $[Ca^{2+}]_r$ (Fig. 1). In MHS muscle fibers $[Ca^{2+}]_r$ increased from 367 ± 5 to 937 ± 6 nM, when $[Na^+]_e$ was reduced to 65 mM and rose to 1,836 ± 8 nM when $[Na^+]_e$ was totally replaced by NMG (Fig. 1).

Removal of Extracellular Ca^{2+} Prevents $[Ca^{2+}]_r$ Increases Induced by Na^+ Depletion—In a different set of experiments we explored the contribution of the Ca^{2+} influx on $[Ca^{2+}]_r$ elevation elicited by Na^+ withdrawal. MHN and MHS swine muscle fibers were incubated for 5 min prior to Na^+ withdrawal in Ca^{2+}-free solution. This exposure significantly reduced $[Ca^{2+}]_r$ in both genotypes, but had a greater effect in MHS than

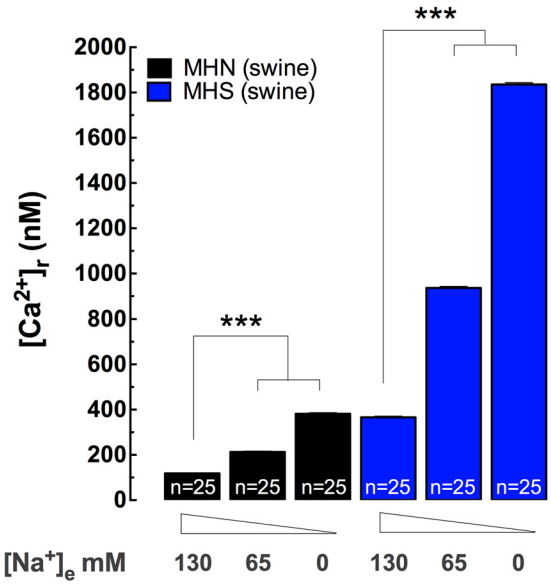

FIGURE 1. **Effect of Na^+ withdrawal on $[Ca^{2+}]_r$ in swine MHN and MHS muscle fibers.** Solutions were prepared replacing NaCl with NMG-HCl. Fibers were incubated 5 min and measurements were assessed by double-barreled selective microelectrodes. Data are expressed as mean ± S.E., $n = 25$ fibers/group, ***, $p < 0.001$; one-way analysis of variance and Tukey's *t* test.

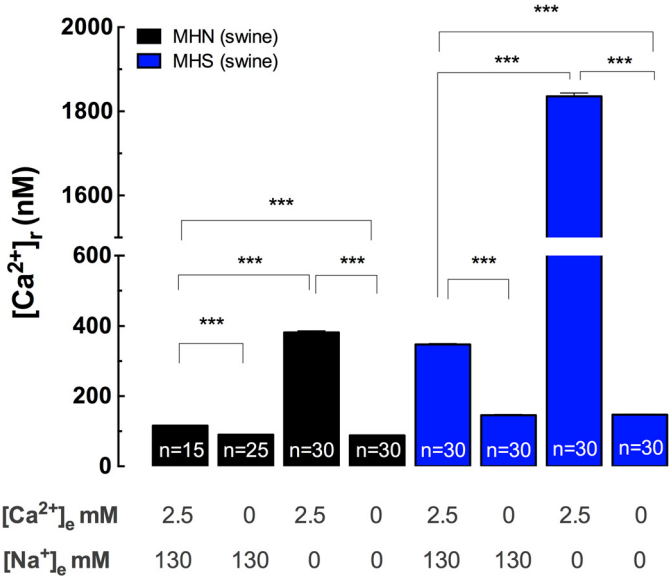

FIGURE 2. **Effect extracellular Ca^{2+} removal on Na^+ depletion-dependent $[Ca^{2+}]_r$ increases.** Swine MHN and MHS muscle fibers were incubated for 5 min in Ca^{2+}-free solution, Na^+-free solution, or Na^+/Ca^{2+}-free solution. $[Ca^{2+}]_r$ was studied with double-barreled selective microelectrodes. Data are expressed as mean ± S.E., n = 15–30 fibers/group, ***, $p < 0.001$; one-way analysis of variance and Tukey's *t* test.

MHN muscles (Fig. 2). In MHN fibers Ca^{2+}-free solution reduced $[Ca^{2+}]_r$ from 116 ± 1 to 90 ± 1 nM and in MHS it was reduced from 348 ± 3 to 146 ± 2 nM. In the absence of extracellular Ca^{2+} the observed raise in $[Ca^{2+}]_r$ elicited by Na^+ withdrawal was completely inhibited in both MHN and MHS muscle fibers (88 ± 1 nM in MHN and 148 ± 1 nM in MHS muscle fibers) (Fig. 2).

T-tubule Disruption Abrogates $[Ca^{2+}]_r$ Increases Induced by Na^+ Withdrawal—To determine the fraction of NCX activity that is restricted to the t-tubules, MHN and MHS muscle fibers

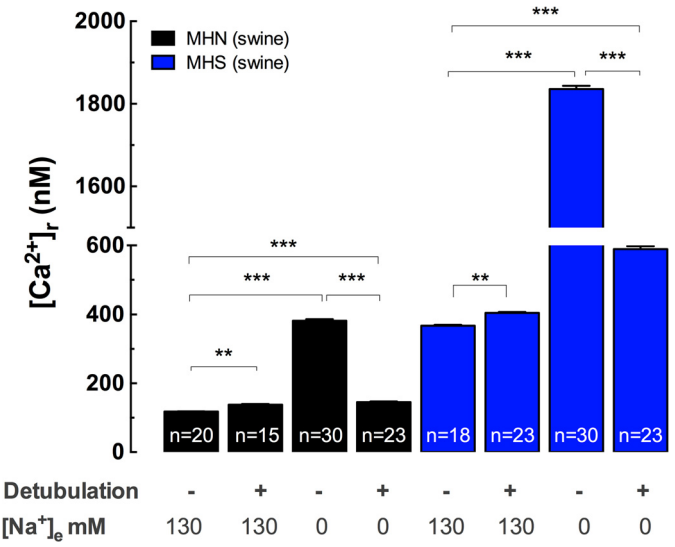

FIGURE 3. **T-tubule disruption modifies $[Ca^{2+}]_r$ increases induced by Na^+ depletion in swine MHN and MHS muscle fibers.** Cells were incubated in 350 mM glycerol solution for 1 h and then returned to swine physiological solution. Ca^{2+} concentrations were determined with double-barreled selective microelectrodes. Data are expressed as mean ± S.E., n = 15–30 fibers/group, **, $p < 0.01$; ***, $p < 0.001$; one-way analysis of variance and Tukey's t test.

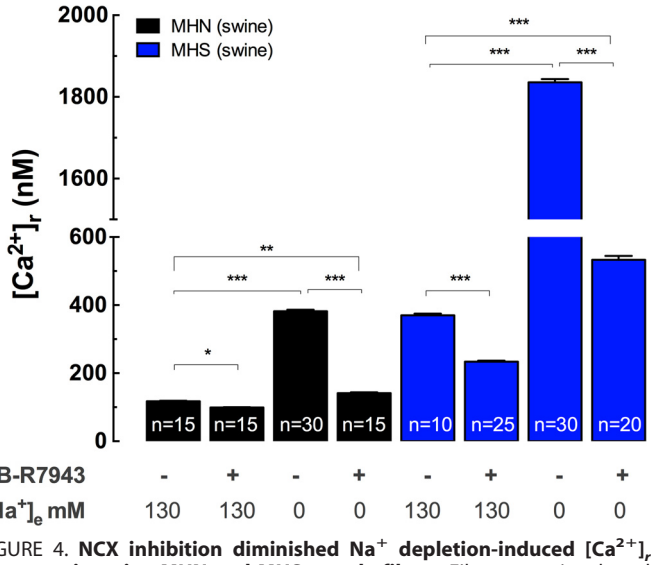

FIGURE 4. **NCX inhibition diminished Na^+ depletion-induced $[Ca^{2+}]_r$ increases in swine MHN and MHS muscle fibers.** Fibers were incubated with the NCX blocker KB-R7943 (10 μM) for 5 min and Ca^{2+} concentrations were determined by selective microelectrodes. Data are expressed as mean ± S.E., n = 10–30 fibers/group; *, $p < 0.05$; **, $p < 0.01$; ***, $p < 0.001$; one-way analysis of variance and Tukey's t test.

were detubulated by a transient osmotic shock with glycerol. $[Ca^{2+}]_r$ was measured during and after hypertonic glycerol treatment and then again after exposure of the detubulated muscle fibers to Na^+-free solution. After glycerol treatment and return to normal swine physiologic solution, $[Ca^{2+}]_r$ in both MHN and MHS fibers rose slightly (Fig. 3). Interestingly, in MHN-glycerol-treated fibers the elevation of $[Ca^{2+}]_r$ elicited by Na^+ withdrawal was reduced to 146 ± 2 nM (382 ± 5 nM, non-treated) and in MHS-glycerol-treated fibers was reduced to 589 ± 9 nM (1,836 ± 8 nM, non-treated) (Fig. 3).

Effects KB-R7943 on $[Ca^{2+}]_r$ in Swine Skeletal Muscle—To clarify mechanisms involved in causing elevation of $[Ca^{2+}]_r$ elicited by exposure to Na^+-free media, the effect of KB-R7943 was studied in MHN and MHS muscle fibers. KB-R7943 acts as a nonspecific blocker of the reverse mode of the NCX3 by modifying the Na^+-dependent binding (35, 36). Preincubation of MHN muscle fibers with 10 μM KB-R7943 reduced $[Ca^{2+}]_r$ from 118 ± 1 to 99 ± 1 nM, and attenuated the increase in $[Ca^{2+}]_r$ associated with exposure to Na^+-free solution (142 ± 2 *versus* 382 ± 5 nM, in the absence of KB-R7943) (Fig. 4). Similarly, KB-R7943 pretreatment of MHS fibers lowered $[Ca^{2+}]_r$ from 370 ± 5 to 234 ± 3 nM and diminished the increase in $[Ca^{2+}]_r$ associated with exposure to Na^+-free solution from 1,836 ± 8 (non-KB-R7943 treated) to 533 ± 11 nM (Fig. 4).

In Vivo $[Ca^{2+}]_r$ and $[Na^+]_r$ Measurements in MHN and MHS Murine Muscle—V_m, $[Ca^{2+}]_r$, and $[Na^+]_r$ were measured *in vivo* in superficial fibers of the vastus lateralis muscle in MHN and MHS mice. $[Ca^{2+}]_r$ observed in MHS muscles was significantly higher than MHN muscles (334 ± 2 *versus* 119 ± 1 nM, $p < 0.001$ n = 20–26), with no difference in resting membrane potential between the two groups (82 ± 0.2 *versus* 82 ± 0.2 mV, $p > 0.05$, n = 20–26). $[Na^+]_r$ was also elevated in MHS compared with MHN (15 ± 0.1 *versus* 8 ± 0.1 mM, $p < 0.001$, n = 15–28).

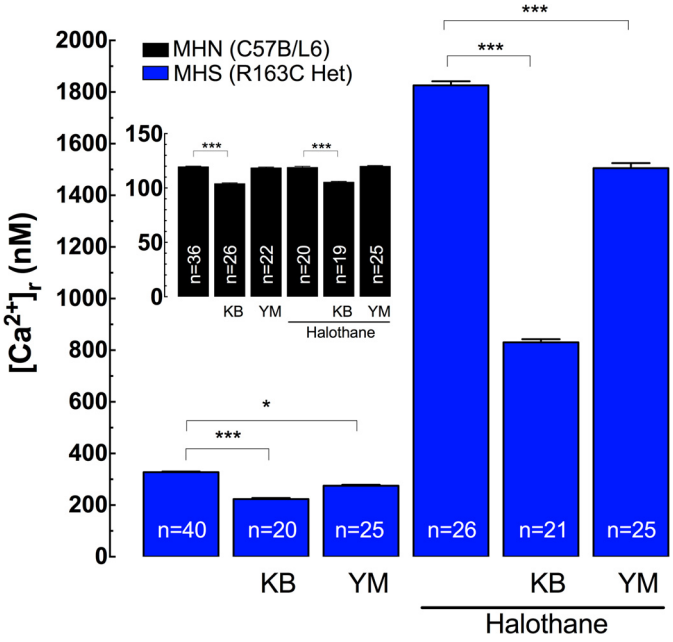

FIGURE 5. **NCX reverse mode blockade modifies halothane-induced $[Ca^{2+}]_r$ increases in MHS murine muscle fibers.** Mice were anesthetized with ketamine and xylazine. KB-R7943 (10 μM) or YM-244769 (1 μM) was added to the perfusion solution directly on vastus lateralis muscle. Halothane (1.5%) was administered using a vaporizer connected to the ventilator. Ca^{2+} concentrations were determined directly into vastus lateralis muscle fibers using double-barreled selective microelectrodes. *Inset* shows $[Ca^{2+}]_r$ in MHN murine muscles. Data are expressed as mean ± S.E., n = 19–40 fibers/group; *, $p < 0.05$; ***, $p < 0.001$; one-way analysis of variance and Tukey's t test.

The Effect of Halothane on $[Ca^{2+}]_r$ and $[Na^+]_r$ in MHS and MHN Murine Muscle in Vivo—Exposure of MHN mice to 1.5% halothane did not produce a significant change in neither V_m nor $[Ca^{2+}]_r$ (Fig. 5, *inset*). However, in MHS muscles, halothane produced a significant elevation of $[Ca^{2+}]_r$ from 327 ± 3 to 1,826 ± 16 nM (Fig. 5) and a small but significant 5-mV depolarization (−77 ± 0.4 mV, n = 26, $p < 0.001$). Simultaneous

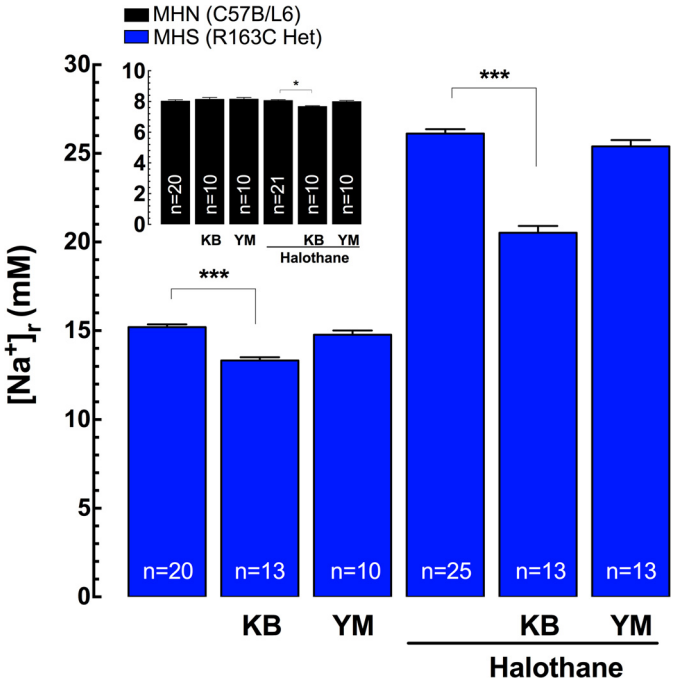

FIGURE 6. **NCX reverse mode blockade modifies halothane-induced $[Na^+]$ increases in MHS murine muscle fibers.** Mice were anesthetized with ketamine and xylazine. KB-R7943 (10 μM) or YM-244769 (1 μM) was added to the perfusion solution directly on vastus lateralis muscle. Halothane (1.5%) was administered using a vaporizer connected to the ventilator. Na^+ concentrations were determined directly into vastus lateralis muscle fibers using double-barreled selective microelectrodes. *Inset* shows $[Na^+]_r$ in MHN murine muscles. Data are expressed as mean ± S.E., $n = 10–25$ fibers/group; ***, $p < 0.001$; one-way analysis of variance and Tukey's *t* test.

recording of $[Na^+]_r$ in the muscle on the opposite leg from that used for $[Ca^{2+}]_r$ measurements showed that 1.5% halothane had no effect on $[Na^+]_r$ in MHN muscle fibers (8 ± 0.1 mM, $p > 0.05$) (Fig. 6, *inset*), but significantly increased $[Na^+]_r$ to 26 ± 0.2 mM ($p < 0.001$) in MHS fibers (Fig. 6).

Effects of KB-R7943 and YM-244769 on $[Ca^{2+}]_r$ in Murine Muscles in Vivo—To determine whether blockade of reverse mode NCX3 with KB-R7943 would modify $[Ca^{2+}]_r$ in murine MHN and MHS quiescent muscle fibers at rest and during halothane exposure, KB-R7943 (10 μM, in murine physiologic solution) was applied locally to superficial fibers of the vastus lateralis muscle for 5 min and then $[Ca^{2+}]_r$ was determined. Incubation with KB-R7943 reduced $[Ca^{2+}]_r$ to 104 ± 1 nM in MHN fibers (Fig. 5, *inset*) and to 224 ± 4 nM in MHS fibers (Fig. 5) but had no effect on V_m in either genotype. In addition, KB-R7943 decreased the elevation of $[Ca^{2+}]_r$ evoked by halothane in MHS muscle fibers from 1,826 ± 16 to 830 ± 12 nM (Fig. 5).

Because KB-R7943 has several targets in the muscle cells, we tested YM-244769 that has high affinity for blocking the reverse mode of NCX3 (37). Exposure of fibers to YM-244769 (1 μM) for 5 min did not modify $[Ca^{2+}]_r$ in MHN fibers (119 ± 1 nM, Fig. 5, *inset*) but reduced $[Ca^{2+}]_r$ to 275 ± 4 nM in MHS fibers (Fig. 5), with no effect V_m in either group. Treatment with YM-244769 also decreased the elevation of $[Ca^{2+}]_r$ observed in MHS muscle fibers caused by halothane from 1,826 ± 16 to 1,505 ± 20 nM (Fig. 5).

TABLE 1
Equilibrium potentials for Na^+, Ca^{2+}, and NCX

Equilibrium potentials were calculated as described under "Experimental Procedures" using the data obtained in this work. V_m, $[Ca^{2+}]_r$, and $[Na^+]_r$ described under "Results" is summarized in the table to allow comparisons.

	MHN		MHS	
	Swine	Murine	Swine	Murine
V_m (mV)	−82	−82	−82	−82
$[Ca^{2+}]_r$ (nM)	119	119	374	334
$[Na^+]_r$ (mM)	8	8	16	15
E_{Na^+} (mV)	+74	+76	+55	+59
$E_{Ca^{2+}}$ (mV)	+132	+132	+117	+118
E_{NCX} (mV)	−42	−36	−69	−59

Effects of KB-R7943 and YM-244769 on $[Na^+]_r$ in Murine Muscle in Vivo—$[Na^+]_r$ was measured on the superficial fibers of vastus lateralis muscles in MHN and MHS murine before and after local application of KB-R7943 or YM-244769 and after exposure to 1.5% halothane vapor in their inspired gas. Local treatment with 10 μM KB-R7943 reduced the $[Na^+]_r$ in MHS murine muscle from 15 ± 0.2 to 13 ± 0.2 mM (Fig. 6), but had no effect in MHN (Fig. 6, *inset*). Local treatment with 1 μM YM-244769 did not modify $[Na^+]_r$ in either genotype (Fig. 6).

Local pretreatment with 10 μM KB-R7943 reduced halothane-induced $[Na^+]_r$ elevation in MHS fibers (21 ± 0.4 *versus* 26 ± 0.2 mM, Fig. 6). On the contrary, YM-244769 had no significant effect on $[Na^+]_r$ in either genotype under any condition tested (Fig. 6).

Equilibrium Potentials—Using the V_m, $[Ca^{2+}]_r$, and $[Na^+]_r$ found in the present study, the Nernst potential for Ca^{2+} ($E_{Ca^{2+}}$) and Na^+ (E_{Na^+}), as well as the reversal or equilibrium potentials for NCX (E_{NCX}) were calculated as described under "Experimental Procedures" and shown in Table 1. We found a difference in the NCX reversal potential of 27 and 23 mV between MHN *versus* MHS from both swine and murine muscle fibers, respectively.

YM-244769 Reduces the Amplitude/Area of the Ca^{2+} Transient Induced by High Potassium in Murine MHS Muscle Fibers—To determine the contribution of the reverse mode of NCX during sustained muscle depolarization, single muscle fibers were exposed to high $[K^+]_e$ in the presence or absence of YM-244769. Fig. 7*A* shows representative fluorescence traces of MHN and MHS murine single fibers loaded with Fluo-4 AM and then exposed to 60 mM $[K^+]_e$ in the presence or absence of 1 μM YM-244769. It can be noticed that Ca^{2+} transient from the MHS muscle fiber is greater (peak and area under the curve) than MHN (Fig. 7*A*), a finding that is consistent with previous observations (34, 38). YM-244769 treatment reduced both the peak amplitude ($\Delta F/F_0$ max) and the area under the curve in MHS fibers, without any significant effect in MHN fibers (Fig. 7, *B* and *C*). Fig. 7*D* shows normalized Ca^{2+} transients (normalization 0 to 1) recorded from single fibers isolated from MHN and MHS with and without YM-244769. YM-244769 also increased the rate of decay of the fluorescence signals in MHS fibers without a significant effect in MHN (Fig. 7*E*).

YM-244769 Does Not Affect SR Ca^{2+} Loading in MHN or MHS Adult Fibers and Myotubes—There was no difference in SR Ca^{2+} loading in MHN or MHS adult FDB fibers after pretreatment with 1 μM YM-244769 and then exposed to caffeine

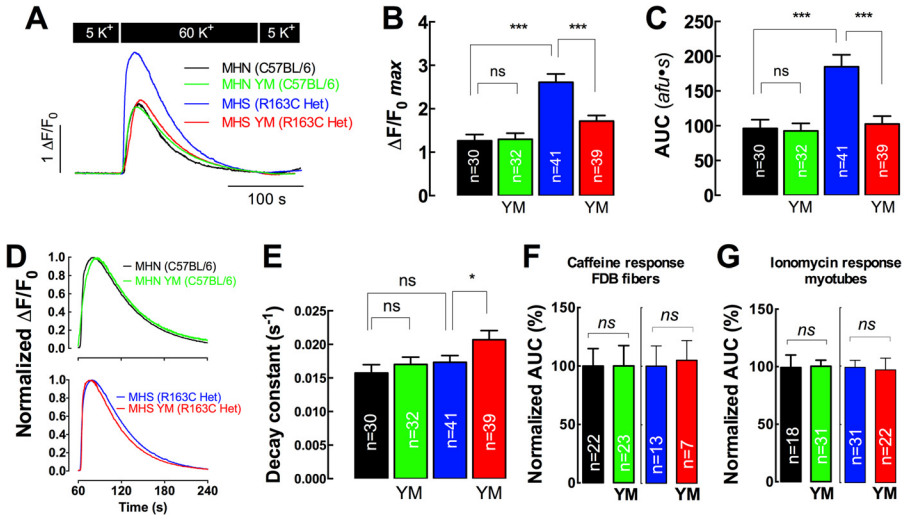

FIGURE 7. **YM-244769 reduces the Ca^{2+} response elicited by high potassium depolarization in adult MHS muscle fibers.** FDB fibers were loaded with Fluo-4 AM (10 μM) for 30 min at room temperature and then exposed to 60 mM extracellular potassium in the presence or absence of YM-244769. *A*, representatives Fluo-4 fluorescence traces in response to extracellular potassium. Amplitude (*B*) and area under curve (*C*) of the obtained Ca^{2+} transients. *D*, normalized Ca^{2+} transients in both MHN and MHS in the presence or absence of YM-244769. The decay of the Ca^{2+} signals were fitted to a single exponential curve and the quantification of the decay constant is shown in *E*. The effect of YM-244769 on SR Ca^{2+} loading was assessed in MHS FDB fibers and myotubes with either caffeine or ionomycin treatment in Ca^{2+}-free media. The area under the curve of the Ca^{2+} transient evoked by caffeine (20 mM) in FDB muscle fibers (*F*) or ionomycin (5 μM) in myotubes (*G*) was calculated under each experimental condition. Data are expressed as mean ± S.E., *n* are indicated in the graph bars. *ns*, no significant; *, $p < 0.05$; ***, $p < 0.001$.

(Fig. 7*F*) or in MHN or MHS myotubes after pre-treatment with 1 μM YM-244769 and perfused with ionomycin (Fig. 7*G*).

NCX3 Expression Is Not Modified in MHS Skeletal Muscle Cells—We measured the level of NCX3 expression by Western blot analysis of total lysates from adult quadriceps muscles and differentiated myotubes. NCX3 expression was similar between MHN and MHS samples ($p = 0.57$ for quadriceps muscles and $p = 0.59$ for myotubes samples) (Fig. 8).

siRNA Knockdown of NCX3 Reduces $[Ca^{2+}]_r$ and the Ca^{2+} Transients Induced by High Potassium in MHS Myotubes—MHN and MHS myotubes were transfected with 25 nM NCX3-siRNA or scramble-FITC-siRNA and then 48 h later the expression levels were assessed by Western blot. Fig. 9*A* shows that NCX3 siRNA significantly reduced expression of the NCX3 protein in both MHN and MHS myotubes compared with scramble-transfected myotubes with a high transfection efficiency (Fig. 9*B*). NCX3 knockdown (48 h) significantly reduced the $[Ca^{2+}]_r$ in MHS myotubes compared with scramble-transfected MHS myotubes (188 ± 6 *versus* 270 ± 8 nM, $p < 0.001$) (Fig. 9*C*). No significant differences in $[Ca^{2+}]_r$ were observed in MHN myotubes transfected with NCX3 siRNA compared with scramble-transfected MHN myotubes. Similarly, we did not observe a significant difference in $[Ca^{2+}]_r$ between scramble-transfected and non-transfected MHN and MHS myotubes (Fig. 9*C*, *dashed horizontal lines* represent the non-transfected $[Ca^{2+}]_r$ levels).

We have previously shown that MHS myotubes had a larger Ca^{2+} transient after exposure to elevated $[K^+]_e$ compared with MHN cells (34, 38). To assess contribution of the NCX3 in the Ca^{2+} response to high $[K^+]_e$, MHN and MHS myotubes were transfected with NCX3 or scramble-siRNA for 48 h and then loaded with Fura-2AM. FITC fluorescence was used to track the transfected myotubes. Fig. 9*D* shows representative Fura-2AM fluorescence traces in transfected myotubes. NCX3

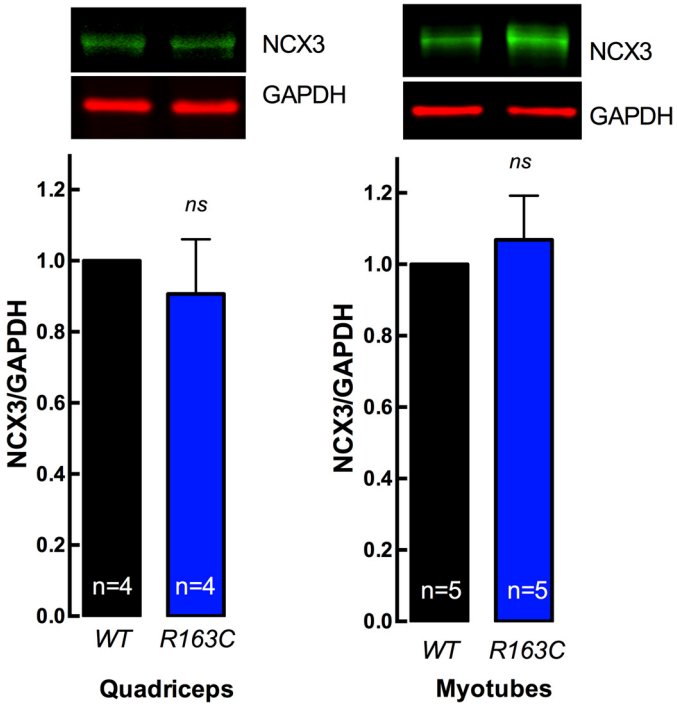

FIGURE 8. **NCX3 expression in MHN and MHS skeletal muscle cells.** Quadriceps muscles were dissected from 3–5-month-old mice and cultured differentiated myotubes from MHN and MHS mice were homogenized and NCX3 protein levels were assessed by Western blot and normalized by GAPDH levels. Data are expressed as mean ± S.E., *n* are indicated in the graph bars. *ns*, no significant difference; unpaired *t* test.

knockdown significantly reduced the amplitude and the transient area in MHS myotubes (Fig. 9, *E* and *F*). However, the effect of NCX3 knockdown in MHN myotubes induced a slightly but significant increase in both the amplitude and area of the evoked transients (Fig. 9, *D–F*). These results suggest that the forward mode NCX is the predominant in MHN myotubes,

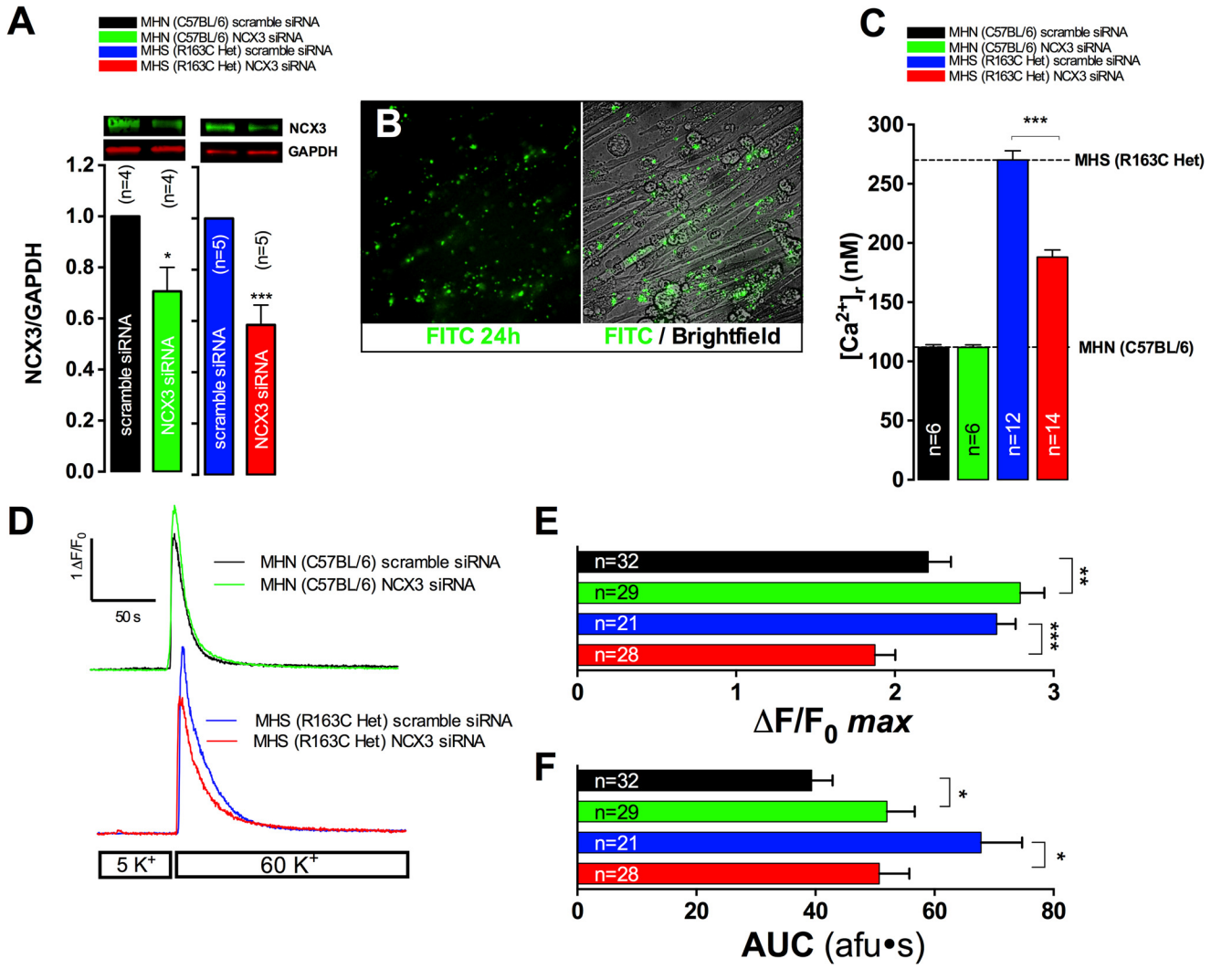

FIGURE 9. **NCX3 knockdown reduced $[Ca^{2+}]_r$ and the calcium response elicited by high potassium depolarization in MHS myotubes.** Myoblasts isolated from MHN and MHS were differentiated for 1 day and then transfected with either scramble- or NCX3-siRNA for 48 h. *A,* NCX3 expression levels in transfected myotubes assessed by Western blot at 48 h. *B,* transfection efficiency was assessed by siRNA FITC fluorescence at 24 h. FITC and Bright Field overlay is shown on the *right panel*. *C,* $[Ca^{2+}]_r$ measurements in both MHN and MHS myotubes after 48 h of transfection. *Dashed horizontal lines* represent the $[Ca^{2+}]_r$ levels in both MHN and MHS untransfected myotubes. *D,* representative Ca^{2+} responses elicited by high potassium depolarization in transfected MHN and MHS myotubes after 48 h. Amplitude (*E*) and area under the curve (*F*) quantification of the recorded Ca^{2+} signals. Data are expressed as mean ± S.E., *n* are indicated in the graph bars. *, $p < 0.05$; **, $p < 0.01$; ***, $p < 0.001$.

contributing to the extrusion of intracellular Ca^{2+} during prolonged depolarization (Fig. 9, *D-F*). These results are supported by the fact that YM-244769 blocks NCX3 in the reverse mode and did not modify the Ca^{2+} transients in MHN (Fig. 7).

DISCUSSION

It is generally accepted that the main pathways of intracellular Ca^{2+} removal in skeletal muscle are: (i) Ca^{2+} uptake via sarcoplasmic reticulum Ca^{2+}-ATPase (39), (ii) Ca^{2+} extrusion via the plasma-membrane Ca^{2+}-ATPase (39), and (iii) Ca^{2+} extrusion by NCX (9, 10, 16). NCX is an electrogenic carrier-mediated transport process that can operate in the forward or reverse mode (2). Perturbation of any of these mechanisms can change the resting intracellular Ca^{2+} regulation in muscle cells.

The present results confirm not only that $[Ca^{2+}]_r$ is elevated in MHS compared with MHN muscle fibers (19, 21, 22), but also that $[Na^+]_r$ is also higher in MHS than MHN (19). $[Na^+]$ is important in modulating intracellular Ca^{2+} concentrations in excitable cells through the NCX. Normally in excitable cells $[Na^+]_r$ is primarily regulated by the Na^+,K^+-ATPase (2), the NCX, and the amiloride-sensitive Na^+/H^+ exchanger (40). An elevated $[Na^+]_r$ would shift the balance of fluxes through NCX to favor more Ca^{2+} influx resulting in an elevation of $[Ca^{2+}]_r$. The elevation of $[Na^+]_r$ found in MHS muscle could be related either to an increased influx or decreased efflux of Na^+. The fact that Na^+,K^+-ATPase expression levels were similar in vastus lateralis from MHS patients who underwent a diagnostic contracture test for susceptibility to malignant hyperthermia (41) and that the values of the V_m in MHN and MHS muscle are similar, suggests that observed dysfunction in $[Na^+]_r$ would most probably be associated with an increase in Na^+ influx rather than a decrease in efflux. In addition, the fact that elevation of $[Na^+]_r$ in murine MHS muscle cells could be attenuated by local application of agents that block Orai1 and nonselective cation entry through transient receptor potential channels 3/6

(TRPC3/6) suggests that the elevation is mediated by an increase in influx of Na^+ and Ca^{2+} through these channels (19). This potential mechanism is supported by a number of electrophysiological studies that demonstrate that TRPCs allow permeation of Na^+ as well as Ca^{2+} (42, 43).

Here we provide evidence that a MH-*RYR1* mutation enhances the reverse mode function of NCX3 in swine and murine skeletal muscle fibers. Withdrawal of external Na^+ ions, which activates the NCX reverse mode (2) caused an increase of $[Ca^{2+}]_r$ in both MHN and MHS swine skeletal muscle not mediated by membrane depolarization, but was more pronounced in MHS muscles. The elevation of $[Ca^{2+}]_r$ was dependent on $[Na^+]_e$. This increase in $[Ca^{2+}]_r$ was reversed in both groups when Na^+ was reintroduced into the physiological solution. The rise in $[Ca^{2+}]_r$ was not associated with membrane depolarization in either MHN or MHS muscle fibers (data not shown). In MHS muscle cells the elevation of $[Ca^{2+}]_r$ elicited by extracellular Na^+ withdrawal produced sarcomere oscillations, which were not seen in MHN cells. This lack of muscle activation in MHN muscle appears to be related to the magnitude of $[Ca^{2+}]_r$ elevation, which fails to reach the mechanical threshold in MHN cells (44, 45). The absence of muscle activation in MHN muscles is in agreement with previous studies where the effect of extracellular Na^+ withdrawal had been studied in diverse muscle preparations (15, 46, 47).

When external Na^+ was replaced with lithium, a classical non-selective NCX blocker (48), a reduction in $[Ca^{2+}]_r$ was observed in both groups (data not shown) supporting the hypothesis that the elevated myoplasmic Ca^{2+} that occurred in the NMG solution was due to the activation of the reverse mode of NCX, rather than a direct effect of NMG on the intracellular Ca^{2+}. The increase in $[Ca^{2+}]_r$ induced by Na^+-free solution has been shown to be enhanced with the blockade of plasma-membrane Ca^{2+}-ATPase with 25 μM carboxyeosin (49, 50) or sarcoplasmic reticulum Ca^{2+}-ATPase with 200 nM 2,5-di(tert-butyl)-1,4-benzohydroquinone (51, 52). These pharmacological treatments also potentiate the observed increase in $[Ca^{2+}]_r$ in swine muscle fibers from both genotypes (data not shown), suggesting that plasma-membrane Ca^{2+}-ATPase as well as sarcoplasmic reticulum Ca^{2+}-ATPase partially buffer the Ca^{2+} influx via the NCX. The source of $[Ca^{2+}]_r$ elevation caused by the Na^+-free solution in MHN and MHS swine muscle fibers appears to be extracellular Ca^{2+}, because incubation of muscle in Ca^{2+}-free solution blocks the elevation of $[Ca^{2+}]_r$ in both genotypes.

Previous work has shown that glycerol treatment disrupts excitation-contraction coupling in skeletal muscle by disconnection of the transverse tubular system from the extracellular space (32, 33). Here we show that detubulation of MHN and MHS swine fibers induces a small increase in $[Ca^{2+}]_r$ in both types of muscle fibers (16% MHN and 10% MHS, respectively). This increment may be related to the change in muscle volume, water moving out the cell, upon exposure to hypertonic solution, because striated muscle behaves as a perfect osmometer, decreasing its volume in proportion to the tonicity of the bathing medium (53, 54). The increase in $[Ca^{2+}]_r$ provoked by Na^+-free solution after muscle detubulation is reduced by 62% in MHN and 68% in MHS compared in non-detubulated muscle fibers. This reduction in the elevation of $[Ca^{2+}]_r$ supports the idea that NCX activity in MHN and MHS muscle fiber appears to be predominantly across the t-tubule rather than the surface sarcolemma. These results agree with previous studies showing that localization of NCX is higher in the t-tubular system than in the sarcolemma in skeletal and cardiac muscles (6, 55).

In the present study KB-R7943 significantly decreases the elevation of $[Ca^{2+}]_r$ provoked by Na^+ withdrawal in MHN (63%) and MHS (71%) swine muscle fibers suggesting that the observed elevation of intracellular $[Ca^{2+}]$ was due to a Ca^{2+} influx mediated by the presence of functional NCX3 in its reverse mode, which appears to be enhanced in MHS muscle cells. Furthermore, this NCX3 blocker reduces $[Ca^{2+}]_r$ by 16 and 37% in MHN and MHS swine muscle, and 13 and 31% in MHN and MHS murine muscles, respectively. However, these reductions in $[Ca^{2+}]_r$ must be considered with caution due to the lack of selectivity of KB-R7943, because there are evidences that show that it also inhibits voltage-gated Na^+ and Ca^{2+} channels, the inward rectifying K^+ channels in cardiac cells (56), the transient receptor potential channels (TRPCs) in HEK293 cells (57), and RyR1 in skeletal muscle and HEK293 cells (58).

On the other hand, YM-244769 is a potent and highly selective NCX blocker that preferentially inhibits the reverse mode of NCX3 (IC_{50} = 18 nM). Furthermore, it is well established that up to 1 μM (dose used in the present study) does not affect the forward mode (37). YM-244769 did not modify $[Ca^{2+}]_r$ in MHN but reduced it by 16% in murine MHS muscle. These results suggest that the reverse mode of NCX3 may play a minor role in the dysregulation of resting intracellular Ca^{2+} observed in quiescent MHS muscle cells. The fact that the effect of YM-244769 on $[Ca^{2+}]_r$ was small compared with KB-R7943 (16 *versus* 37%) is consistent with the fact that KB-R7943 may be blocking several Ca^{2+} entry pathways as described above. We have shown *in vivo* that exposure of MHS muscle fibers to halothane caused a robust elevation on intracellular $[Ca^{2+}]$ (19, 22). Local application of KB-R7943 and YM-244769 reduced the elevation of $[Ca^{2+}]_r$ induced by halothane *in vivo* by 55 and 18%, respectively, in MHS murine muscle fibers. This difference in the reduction of intracellular $[Ca^{2+}]$ upon halothane exposure (55 *versus* 18%) may be related to the specificity of the agents regarding their pharmacological effects. Taken together, these data strongly support the hypothesis that sarcolemmal Ca^{2+} entry mediated by the reverse mode of NCX3 (reported here) in combination with Gd^{3+}- or GsTMX4-sensitive pathways (19) plays an important role in maintaining the new steady-state for $[Ca^{2+}]_r$ observed during an MH episode triggered by halothane.

Previous reports have shown that skeletal muscle fibers can contract after electrical stimulation or under whole cell voltage clamp with short step depolarization in low extracellular Ca^{2+} concentrations (59, 60). However, the importance of extracellular Ca^{2+} both in the presence (61, 62) and absence of Ca^{2+} buffers (63) for maintenance of muscle K^+ contractures has also been well demonstrated. However, our data provide evidence that extracellular Ca^{2+} influx mediated by the reverse mode of NCX3 plays a role for the maintenance of Ca^{2+} transients induced by elevated $[K^+]_e$ in MHS muscle fibers. In fact, the peak amplitude and area were reduced and duration of the Ca^{2+} transient elicited by $[K^+]_e$ was shortened (increased rate of decay of peak Ca^{2+}) in the presence of YM-244769. These

pharmacological effects are not mediated by a reduction in SR Ca^{2+} loading in either MHN or MHS fibers. Our experiments in FDB fibers challenged with caffeine and in myotubes challenged with ionomycin showed that YM-244769 did not modify SR Ca^{2+} loading. The fact that we did not observe a significant reduction in the peak Ca^{2+} transient amplitude, in the area under the curve or rate of decay in MHN fibers in the presence of YM-244769 suggest that the reverse mode of NCX3 plays little or no role in MHN muscle fibers during sustained depolarization. Our pharmacologic observations are supported by our findings using siRNA knockdown of NCX3 in MHS myotubes, which both reduced the $[Ca^{2+}]_r$ and the amplitude/area of the Ca^{2+} transient induced by high extracellular potassium confirming the role of Ca^{2+} entry mediated by NCX3 at rest and during sustained depolarization.

The increased NCX3 reverse mode activity in MHS murine muscle cells suggest a compensatory mechanism to overcome the lower SR Ca^{2+} loading described in MHS muscle cells (19, 25, 64) as a result of RyR1-MH leakiness (21). The reduced SR Ca^{2+} levels are likely to promote an increased Ca^{2+} influx through Orai and TRPC channels (19), and possibly other Ca^{2+} channels (34). Our previously published data indicated that depolarization with 60 mM K^+ produced an average area under the curve of the Ca^{2+} transient ≈2-fold greater in myotubes from heterozygous MHS R163C compared with WT myotubes (34). Extracellular Ca^{2+} plays a significant physiological role for the maintenance of Ca^{2+} transients induced by elevated $[K^+]_e$ in WT and R163C MHS myotubes, with a more pronounced effect in the later (34).

It is very well established that the direction in which NCX works is determined largely by the relative electrochemical driving forces for Na^+ and Ca^{2+} ions and the resting membrane potential. If the driving force for three Na^+ into the cell is larger than that for one Ca^{2+} into the cell (3:1 Na^+/Ca^{2+} stoichiometry), the exchanger will transport Na^+ ions into the cell and take Ca^{2+} ions out (forward mode). On the other hand, if under another set of conditions (altered membrane potential, ionic gradients, or post-translational modifications), the driving force for three Na^+ into the cell is less than for one Ca^{2+} into the cell, then the Ca^{2+} electrochemical gradient will become the dominant inward driving force (reverse mode). The present results show that in MHS muscle the NCX reverse potential (E_{NCX}) shifts to a more negative value. In swine it shifts from −42 mV in MHN to −69 mV in MHS and in mice from −36 mV in MHN to −59 mV in MHS muscle cells. These shifts in E_{NCX} (+27 and +23 mV) observed in MHS muscle cells imply a major Ca^{2+} influx via reverse mode of NCX with muscle depolarization. The net effect will be an increase in the intracellular Ca^{2+} concentration during muscle activation.

In summary, these results provide evidence that both swine and murine muscle fibers possess a functional NCX, which can mediate Ca^{2+} entry when the Na^+ electrochemical gradient is reduced (reverse mode). This Ca^{2+} entry via the reverse mode was greater in MHS than MHN muscles, and is sensitive to NCX3 blockers like KB-R7943 and YM-244769. Furthermore, the reverse mode of NCX3 contributes to the overall Ca^{2+} elevation observed during sustained depolarization induced by high $[K^+]_e$ and MH episode elicited by halothane.

Acknowledgment—We are grateful to Dr. Takahiro Iwamoto for providing YM-244769 NCX blocker.

REFERENCES

1. Philipson, K. D., and Nicoll, D. A. (2000) Sodium-calcium exchange: a molecular perspective. *Annu. Rev. Physiol.* **62,** 111–133
2. Blaustein, M. P., and Lederer, W. J. (1999) Sodium/calcium exchange: its physiological implications. *Physiol. Rev.* **79,** 763–854
3. Yu, A. S., Hebert, S. C., Lee, S. L., Brenner, B. M., and Lytton, J. (1992) Identification and localization of renal Na^+-Ca^{2+} exchanger by polymerase chain reaction. *Am. J. Physiol.* **263,** F680–685
4. Nicoll, D. A., Quednau, B. D., Qui, Z., Xia, Y. R., Lusis, A. J., and Philipson, K. D. (1996) Cloning of a third mammalian Na^+-Ca^{2+} exchanger, NCX3. *J. Biol. Chem.* **271,** 24914–24921
5. Li, Z., Matsuoka, S., Hryshko, L. V., Nicoll, D. A., Bersohn, M. M., Burke, E. P., Lifton, R. P., and Philipson, K. D. (1994) Cloning of the NCX2 isoform of the plasma membrane Na^+-Ca^{2+} exchanger. *J. Biol. Chem.* **269,** 17434–17439
6. Sacchetto, R., Margreth, A., Pelosi, M., and Carafoli, E. (1996) Colocalization of the dihydropyridine receptor, the plasma-membrane calcium ATPase isoform 1 and the sodium/calcium exchanger to the junctional-membrane domain of transverse tubules of rabbit skeletal muscle. *Eur. J. Biochem.* **237,** 483–488
7. Deval, E., Levitsky, D. O., Marchand, E., Cantereau, A., Raymond, G., and Cognard, C. (2002) Na^+/Ca^{2+} exchange in human myotubes: intracellular calcium rises in response to external sodium depletion are enhanced in DMD. *Neuromuscul. Disord.* **12,** 665–673
8. Fraysse, B., Rouaud, T., Millour, M., Fontaine-Pérus, J., Gardahaut, M. F., and Levitsky, D. O. (2001) Expression of the Na^+/Ca^{2+} exchanger in skeletal muscle. *Am. J. Physiol. Cell Physiol.* **280,** C146-C154
9. Caputo, C., and Bolaños, P. (1978) Effect of external sodium and calcium on calcium efflux in frog striated muscle. *J. Membr. Biol.* **41,** 1–14
10. Cifuentes, F., Vergara, J., and Hidalgo, C. (2000) Sodium/calcium exchange in amphibian skeletal muscle fibers and isolated transverse tubules. *Am. J. Physiol. Cell Physiol.* **279,** C89-C97
11. Gilbert, J. R., and Meissner, G. (1982) Sodium-calcium ion exchange in skeletal muscle sarcolemmal vesicles. *J. Membr. Biol.* **69,** 77–84
12. Hidalgo, C., Cifuentes, F., and Donoso, P. (1991) Sodium-calcium exchange in transverse tubule vesicles isolated from amphibian skeletal muscle. *Ann. N.Y. Acad. Sci.* **639,** 483–497
13. Donoso, P., and Hidalgo, C. (1989) Sodium-calcium exchange in transverse tubules isolated from frog skeletal muscle. *Biochim. Biophys. Acta* **978,** 8–16
14. Castillo, E., Gonzalez-Serratos, H., Rasgado-Flores, H., and Rozycka, M. (1991) Na-Ca exchange studies in frog phasic muscle cells. *Ann. N.Y. Acad. Sci.* **639,** 554–557
15. Garcia, M. C., Diaz, A. F., Godinez, R., and Sanchez, J. A. (1992) Effect of sodium deprivation on contraction and charge movement in frog skeletal muscle fibres. *J. Muscle Res. Cell Motil.* **13,** 354–365
16. Gonzalez-Serratos, H., Hilgemann, D. W., Rozycka, M., Gauthier, A., and Rasgado-Flores, H. (1996) Na-Ca exchange studies in sarcolemmal skeletal muscle. *Ann. N.Y. Acad. Sci.* **779,** 556–560
17. Muñiz, J., Huerta, M., Marin, J. L., and Vásquez, C. (1991) Sodium withdrawal contractures in tonic skeletal muscle fibers of the frog. *Ann. N.Y. Acad. Sci.* **639,** 573–575
18. Nelson, T. E. (2002) Malignant hyperthermia: a pharmacogenetic disease of Ca^{2+} regulating proteins. *Curr. Mol. Med.* **2,** 347–369
19. Eltit, J. M., Ding, X., Pessah, I. N., Allen, P. D., and Lopez, J. R. (2013) Nonspecific sarcolemmal cation channels are critical for the pathogenesis of malignant hyperthermia. *FASEB J.* **27,** 991–1000
20. López, J. R., Alamo, L., Caputo, C., Wikinski, J., and Ledezma, D. (1985) Intracellular ionized calcium concentration in muscles from humans with malignant hyperthermia. *Muscle Nerve* **8,** 355–358
21. Yang, T., Esteve, E., Pessah, I. N., Molinski, T. F., Allen, P. D., and López, J. R. (2007) Elevated resting $[Ca^{2+}]_i$ in myotubes expressing malignant hyperthermia RyR1 cDNAs is partially restored by modulation of passive

calcium leak from the SR. *Am. J. Physiol. Cell Physiol.* **292,** C1591–1598
22. López, J. R., Allen, P. D., Alamo, L., Jones, D., and Sreter, F. A. (1988) Myoplasmic free [Ca^{2+}] during a malignant hyperthermia episode in swine. *Muscle Nerve* **11,** 82–88
23. Iaizzo, P. A., Klein, W., and Lehmann-Horn, F. (1988) Fura-2 detected myoplasmic calcium and its correlation with contracture force in skeletal muscle from normal and malignant hyperthermia susceptible pigs. *Pflugers Arch.* **411,** 648–653
24. Robinson, R., Carpenter, D., Shaw, M. A., Halsall, J., and Hopkins, P. (2006) Mutations in RYR1 in malignant hyperthermia and central core disease. *Hum. Mutat.* **27,** 977–989
25. Eltit, J. M., Bannister, R. A., Moua, O., Altamirano, F., Hopkins, P. M., Pessah, I. N., Molinski, T. F., López, J. R., Beam, K. G., and Allen, P. D. (2012) Malignant hyperthermia susceptibility arising from altered resting coupling between the skeletal muscle L-type Ca^{2+} channel and the type 1 ryanodine receptor. *Proc. Natl. Acad. Sci. U.S.A.* **109,** 7923–7928
26. Jurkat-Rott, K., McCarthy, T., and Lehmann-Horn, F. (2000) Genetics and pathogenesis of malignant hyperthermia. *Muscle Nerve* **23,** 4–17
27. Monnier, N., Procaccio, V., Stieglitz, P., and Lunardi, J. (1997) Malignant-hyperthermia susceptibility is associated with a mutation of the α1-subunit of the human dihydropyridine-sensitive L-type voltage-dependent calcium-channel receptor in skeletal muscle. *Am. J. Hum. Genet.* **60,** 1316–1325
28. Vogeli, P., Bolt, R., Fries, R., and Stranzinger, G. (1994) Co-segregation of the malignant hyperthermia and the Arg^{615}-Cys^{615} mutation in the skeletal muscle calcium release channel protein in five European Landrace and Pietrain pig breeds. *Anim. Genet.* **25,** 59–66
29. Yang, T., Riehl, J., Esteve, E., Matthaei, K. I., Goth, S., Allen, P. D., Pessah, I. N., and Lopez, J. R. (2006) Pharmacologic and functional characterization of malignant hyperthermia in the R163C RyR1 knock-in mouse. *Anesthesiology* **105,** 1164–1175
30. López, J. R., Alamo, L., Caputo, C., DiPolo, R., and Vergara, S. (1983) Determination of ionic calcium in frog skeletal muscle fibers. *Biophys. J.* **43,** 1–4
31. Edman, K. A., and Flitney, F. W. (1982) Laser diffraction studies of sarcomere dynamics during "isometric" relaxation in isolated muscle fibres of the frog. *J. Physiol.* **329,** 1–20
32. Davey, D. F., Dulhunty, A. F., and Fatkin, D. (1980) Glycerol treatment in mammalian skeletal muscle. *J. Membr. Biol.* **53,** 223–233
33. Eisenberg, B., and Eisenberg, R. S. (1968) Transverse tubular system in glycerol-treated skeletal muscle. *Science* **160,** 1243–1244
34. Estève, E., Eltit, J. M., Bannister, R. A., Liu, K., Pessah, I. N., Beam, K. G., Allen, P. D., and López, J. R. (2010) A malignant hyperthermia-inducing mutation in RYR1 (R163C): alterations in Ca^{2+} entry, release, and retrograde signaling to the DHPR. *J. Gen. Physiol.* **135,** 619–628
35. Akabas, M. H. (2004) Na^+/Ca^{2+} exchange inhibitors: potential drugs to mitigate the severity of ischemic injury. *Mol. Pharmacol.* **66,** 8–10
36. Iwamoto, T., Watano, T., and Shigekawa, M. (1996) A novel isothiourea derivative selectively inhibits the reverse mode of Na^+/Ca^{2+} exchange in cells expressing NCX1. *J. Biol. Chem.* **271,** 22391–22397
37. Iwamoto, T., and Kita, S. (2006) YM-244769, a novel Na^+/Ca^{2+} exchange inhibitor that preferentially inhibits NCX3, efficiently protects against hypoxia/reoxygenation-induced SH-SY5Y neuronal cell damage. *Mol. Pharmacol.* **70,** 2075–2083
38. Yang, T., Allen, P. D., Pessah, I. N., and Lopez, J. R. (2007) Enhanced excitation-coupled calcium entry in myotubes is associated with expression of RyR1 malignant hyperthermia mutations. *J. Biol. Chem.* **282,** 37471–37478
39. Wuytack, F., Raeymaekers, L., De Smedt, H., Eggermont, J. A., Missiaen, L., Van Den Bosch, L., De Jaegere, S., Verboomen, H., Plessers, L., and Casteels, R. (1992) Ca^{2+}-transport ATPases and their regulation in muscle and brain. *Ann. N.Y. Acad. Sci.* **671,** 82–91
40. Juel, C. (1995) Regulation of cellular pH in skeletal muscle fiber types, studied with sarcolemmal giant vesicles obtained from rat muscles. *Biochim. Biophys. Acta* **1265,** 127–132
41. Everts, M. E., Ording, H., Hansen, O., and Nielsen, P. A. (1992) Ca^{2+}-ATPase and Na^+-K^+-ATPase content in skeletal muscle from malignant hyperthermia patients. *Muscle Nerve* **15,** 162–167
42. Hofmann, T., Obukhov, A. G., Schaefer, M., Harteneck, C., Gudermann, T., and Schultz, G. (1999) Direct activation of human TRPC6 and TRPC3 channels by diacylglycerol. *Nature* **397,** 259–263
43. Hurst, R. S., Zhu, X., Boulay, G., Birnbaumer, L., and Stefani, E. (1998) Ionic currents underlying HTRP3 mediated agonist-dependent Ca^{2+} influx in stably transfected HEK293 cells. *FEBS Lett.* **422,** 333–338
44. Ford, L. E., and Podolsky, R. J. (1972) Intracellular calcium movements in skinned muscle fibres. *J. Physiol.* **223,** 21–33
45. Godt, R. E. (1974) Calcium-activated tension of skinned muscle fibers of the frog. Dependence on magnesium adenosine triphosphate concentration. *J. Gen. Physiol.* **63,** 722–739
46. Kawata, H., and Fujishiro, N. (1990) Effects of sodium depletion on the caffeine-induced contraction of frog's skeletal muscle. *Jpn. J. Physiol.* **40,** 243–251
47. Même, W., and Léoty, C. (1999) Na^+-Ca^{2+} exchange induces low Na^+ contracture in frog skeletal muscle fibers after partial inhibition of sarcoplasmic reticulum Ca^{2+}-ATPase. *Pflugers Arch.* **438,** 851–859
48. Miura, Y., and Kimura, J. (1989) Sodium-calcium exchange current. Dependence on internal Ca and Na and competitive binding of external Na and Ca. *J. Gen. Physiol.* **93,** 1129–1145
49. Mackiewicz, U., Maczewski, M., Konior, A., Tellez, J. O., Nowis, D., Dobrzynski, H., Boyett, M. R., and Lewartowski, B. (2009) Sarcolemmal Ca^{2+}-ATPase ability to transport Ca2+ gradually diminishes after myocardial infarction in the rat. *Cardiovasc. Res.* **81,** 546–554
50. Wanaverbecq, N., Marsh, S. J., Al-Qatari, M., and Brown, D. A. (2003) The plasma membrane calcium-ATPase as a major mechanism for intracellular calcium regulation in neurones from the rat superior cervical ganglion. *J. Physiol.* **550,** 83–101
51. Nakamura, H., Nakasaki, Y., Matsuda, N., and Shigekawa, M. (1992) Inhibition of sarcoplasmic reticulum Ca^{2+}-ATPase by 2,5-di(tert-butyl)-1,4-benzohydroquinone. *J. Biochem.* **112,** 750–755
52. Wictome, M., Michelangeli, F., Lee, A. G., and East, J. M. (1992) The inhibitors thapsigargin and 2,5-di(tert-butyl)-1,4-benzohydroquinone favour the E2 form of the Ca^{2+},Mg^{2+}-ATPase. *FEBS Lett.* **304,** 109–113
53. Blinks, J. R. (1965) Influence of osmotic strength on cross-section and volume of isolated single muscle fibres. *J. Physiol.* **177,** 42–57
54. Hodgkin, A. L., and Horowicz, P. (1957) Effects of K and Cl on the membrane potential of isolated muscle fibres. *J. Physiol.* **137,** 30P
55. Despa, S., Brette, F., Orchard, C. H., and Bers, D. M. (2003) Na/Ca exchange and Na/K-ATPase function are equally concentrated in transverse tubules of rat ventricular myocytes. *Biophys. J.* **85,** 3388–3396
56. Watano, T., Kimura, J., Morita, T., and Nakanishi, H. (1996) A novel antagonist, No. 7943, of the Na^+/Ca^{2+} exchange current in guinea-pig cardiac ventricular cells. *Br. J. Pharmacol.* **119,** 555–563
57. Kraft, R. (2007) The Na^+/Ca^{2+} exchange inhibitor KB-R7943 potently blocks TRPC channels. *Biochem. Biophys. Res. Commun.* **361,** 230–236
58. Barrientos, G., Bose, D. D., Feng, W., Padilla, I., and Pessah, I. N. (2009) The Na^+/Ca^{2+} exchange inhibitor 2-(2-(4-(4-nitrobenzyloxy)phenyl) ethyl)isothiourea methanesulfonate (KB-R7943) also blocks ryanodine receptors type 1 (RyR1) and type 2 (RyR2) channels. *Mol. Pharmacol.* **76,** 560–568
59. Armstrong, C. M., Bezanilla, F. M., and Horowicz, P. (1972) Twitches in the presence of ethylene glycol bis(-aminoethyl ether)-*N,N′*-tetracetic acid. *Biochim. Biophys. Acta* **267,** 605–608
60. Bolaños, P., Caputo, C., and Velaz, L. (1986) Effects of calcium, barium and lanthanum on depolarization-contraction coupling in skeletal muscle fibres of *Rana pipiens*. *J. Physiol.* **370,** 39–60
61. Cota, G., and Stefani, E. (1981) Effects of external calcium reduction on the kinetics of potassium contractures in frog twitch muscle fibres. *J. Physiol.* **317,** 303–316
62. Lüttgau, H. C., and Spiecker, W. (1979) The effects of calcium deprivation upon mechanical and electrophysiological parameters in skeletal muscle fibres of the frog. *J. Physiol.* **296,** 411–429
63. Caputo, C., and Gimenez, M. (1967) Effects of external calcium deprivation on single muscle fibers. *J. Gen. Physiol.* **50,** 2177–2195
64. Manno, C., Figueroa, L., Royer, L., Pouvreau, S., Lee, C. S., Volpe, P., Nori, A., Zhou, J., Meissner, G., Hamilton, S. L., and Ríos, E. (2013) Altered Ca^{2+} concentration, permeability and buffering in the myofibre Ca^{2+} store of a mouse model of malignant hyperthermia. *J. Physiol.* **591,** 4439–4457